# Chapter 6
# A Review of Uncertainty in Data Visualization

**Ken Brodlie, Rodolfo Allendes Osorio, and Adriano Lopes**

**Abstract** Most visualization techniques have been designed on the assumption that the data to be represented are free from uncertainty. Yet this is rarely the case. Recently the visualization community has risen to the challenge of incorporating an indication of uncertainty into visual representations, and in this article we review their work. We place the work in the context of a reference model for data visualization, that sees data pass through a pipeline of processes. This allows us to distinguish the *visualization of uncertainty*—which considers how we depict uncertainty specified with the data—and the *uncertainty of visualization*—which considers how much inaccuracy occurs as we process data through the pipeline. It has taken some time for uncertain visualization methods to be developed, and we explore why uncertainty visualization is hard—one explanation is that we typically need to find another display dimension and we may have used these up already! To organize the material we return to a typology developed by one of us in the early days of visualization, and make use of this to present a catalog of visualization techniques describing the research that has been done to extend each method to handle uncertainty. Finally we note the responsibility on us all to incorporate any known uncertainty into a visualization, so that integrity of the discipline is maintained.

## 6.1 Introduction

Understanding uncertainty is one of the great scientific challenges of our time. It impacts on many crucial issues facing the world today—from climate change

K. Brodlie (✉)
University of Leeds, Leeds LS2 9JT, UK
e-mail: k.w.brodlie@leeds.ac.uk

R. Allendes Osorio
Depto. de Ciencias de la Computación, Fac. de Ingeneria, Universidad de Talca, Talca, Chile
e-mail: rallendes@utalca.cl

A. Lopes
CITI / Depto. Informática, FCT, Universidade Nova de Lisboa, Lisbon, Portugal
e-mail: alopes@fct.unl.pt

J. Dill et al. (eds.), *Expanding the Frontiers of Visual Analytics and Visualization*,
DOI 10.1007/978-1-4471-2804-5_6, 

prediction, to economic modeling, to interpretation of medical data. Visualization is now well accepted as a powerful means to allow scientists to explore large datasets, and to present their results to a wider audience. Yet most visualization techniques make the assumption that the data they are displaying are *exact*. We may encounter error bars on graphs, but we rarely see the equivalent on contour maps or isosurfaces. Indeed the very crispness of an isosurface gives an impression of confidence that is frankly often an illusion. This is a major issue when visualizations are used in decision making—such as planning evacuations based on a visualization of the predicted hurricane path. Indeed as computation power and capability continue to increase we see a rise in *ensemble computing*, where many simulations of a phenomenon are carried out for different initial conditions, or different settings of unknown parameters—leading not to a unique data value, but to a set of values—so-called multivalue data. There is a growing awareness of the uncertainty problem within the visualization community, and many traditional techniques are being extended to represent not only the data, but also the uncertainty information associated with the data. We call this *visualization of uncertainty*. In addition it is important to realize that, even if there is certainty about the data, errors can occur in the process of turning the data into a picture. We call this *uncertainty of visualization*. In this paper we aim to review the current state of the art in uncertainty in scientific visualization, looking at both of these aspects.

There are a growing number of application areas where uncertainty visualization is being put to good effect. Here is a brief list, together with relevant citations: agriculture (Juang et al. 2004); astrophysics (Li et al. 2007); biology (Cumming et al. 2007); climate studies (Pöthkow et al. 2011; Potter et al. 2009); fluid flow (Botchen et al. 2005; Hlawatsch et al. 2011; Otto et al. 2010; Wittenbrink et al. 1996; Zuk et al. 2008); geography (Aerts et al. 2003; Davis and Keller 1997; Ehlschlaeger et al. 1997; Goodchild et al. 1994; Hengl 2003; Love et al. 2005; MacEachren 1992; MacEachren et al. 2005); geophysics (Zehner et al. 2010); medicine (Kniss et al. 2005; Lundstrom et al. 2007; Prabni et al. 2010); meteorology (Boller et al. 2010; Luo et al. 2003; Sanyal et al. 2010); oceanography (Allendes Osorio and Brodlie 2008; Bingham and Haines 2006; Djurcilov et al. 2002); underground assets (Boukhelifa and Duke 2007); visual analytics (Correa et al. 2009).

Historically the geovisualization community were perhaps the first to realize the importance of uncertainty. This community have long been concerned with issues of data quality so that the limitations of the data are understood when looking at maps. Buttenfield and Beard (1994) suggested that:

> Computer generated maps, a standard output of GIS, generally imply an accuracy not warranted by the data.

The paper by Goodchild et al. (1994) presents a view of the 1994 state of art in visualizing data validity, while MacEachren et al. (2005) provides a view of the field in 2005. Interest within the scientific visualization community developed rather later: the paper by Pang et al. (1997) provides possibly the first significant review of the field. Important subsequent reviews include the papers by Griethe and Schumann (2006) and by Zuk and Carpendale (2006) (who look at the area from the perspective

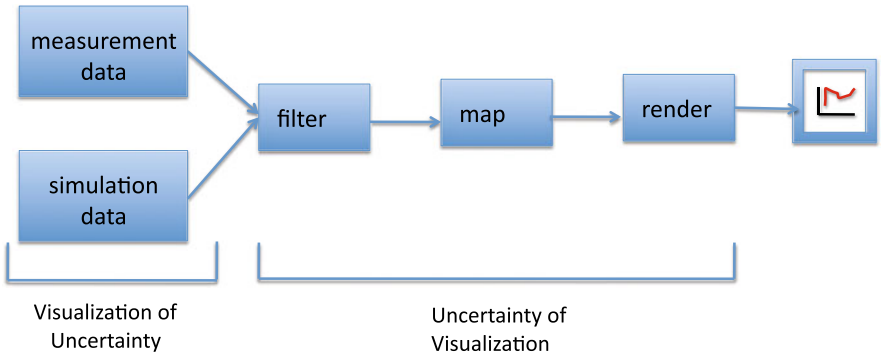


**Fig. 6.1** Haber and McNabb model: visualization of uncertainty and uncertainty of visualization

of perceptual theory and in particular the work of Bertin, Tufte and Ware), while important awareness-raising papers are Johnson and Sanderson (2003) and Johnson (2004) who includes the representation of error and uncertainty as one of his top ten research problems. Recent theses include those of Allendes Osorio (2010) and Zuk (2008).

The structure of our review is as follows. We begin in Sect. 6.2 with a reference model for uncertainty visualization that can help us understand where uncertainty occurs in visualization. We then reflect in Sect. 6.3 on why visualization of uncertainty, and uncertainty of visualization, are hard problems. We then organize the main body of the review under a classification similar to that introduced by Brodlie et al. (1992) and used and extended by Pang et al. (1997) in their review. Section 6.4 introduces the notation and is followed by two sections: Sect. 6.5 focuses on visualization of uncertain data, where most of the research has been done; and Sect. 6.6 looks at the uncertainty of visualization.

## 6.2 Uncertainty Reference Model

We can understand the different sources of uncertainty by re-visiting the visualization reference model presented by Haber and McNabb (1990). In Fig. 6.1, we show the traditional model of data passing through a pipeline. The first step is to filter, or reconstruct through interpolation or approximation, creating a model of the entity underlying the data. This model is then passed to a mapping stage, where a visualization algorithm produces geometry. Finally this geometry is rendered as an image. Uncertainty occurs at all stages—visualization of uncertainty focuses on the data stage, while the uncertainty of visualization begins at the filter stage and passes through to the render stage.

**data** The source of the data may be measurement or simulation. In either case, the data may have associated uncertainty information—this may be in the form of a known range of error; or the data may be described as a random variate with a

given probability distribution; or the data may be multi-valued as a result of an ensemble of simulations or multiple measurements.

**filter** The filtering stage builds an empirical model from the data—we are making plausible inferences from incomplete information. In the case of exact data, the empirical model is typically created by *interpolation*—calculating a curve, surface or volume *through* the given data. Of course uncertainty is introduced here because we are only guessing at the behavior between data points. When we have uncertain data, then a different approach is needed. One option is to take a representative value at each datapoint (this might be the mean if several possible values are given), and to associate with it a measure of the uncertainty (perhaps a standard deviation); the representative is then used as though it were exact, and interpolation used to create an empirical model, but with the associated uncertainty model attached to it. A variation of this is to estimate the distribution at a datapoint as a Probability Density Function (PDF), and build an empirical model as an interpolation of these PDFs. A different option, if we have prior knowledge of the form of the model, is to fit a parameterized form of the model to the data forming in some sense a best *approximation*—for example, if the model is linear, then linear regression would be appropriate; more generally, spline data-fitting using least-squares will enable a useful approximation to be constructed. The *E*02 chapter of the NAG Library is a good source of software for data fitting (www.nag.co.uk). This second option of data fitting has not been the focus of the recent uncertainty visualization research, and so we shall not discuss it further here—but it remains a very important practical approach.

**map** The map process, or visualization algorithm, where a geometric model is created, may involve computation that is subject to error—for example the approximation of curved surfaces by polygons, or the creation of streamlines by numerical solution of ordinary differential equations.

**render** The render process which rasterizes the geometry involves a discretization step that may hide information—for example if the resolution of the output image is of a lower order of magnitude than the resolution of the data. Here focus and context ideas might usefully be employed to overcome this difficulty.

Other authors have similarly used the Haber and McNabb model as a reference for uncertainty, including Pang et al. (1997), Griethe and Schumann (2006), Lopes and Brodlie (1999), Correa et al. (2009).

We tend to see the pipeline as a left-to-right output process, with uncertainty accumulating as data passes through. In interactive work, we also traverse the model from right-to-left, and uncertainty needs to be borne in mind as we pass back along the pipeline.

## 6.3 Why Is Uncertainty so Hard?

Most visualization techniques have been developed, and used, under an assumption that the given data are exact—and any uncertainty information is not included in the

picture. While this situation is changing, it has taken a long time. Why is uncertainty a hard topic in visualization? Here are some possible explanations:

**Uncertainty is complex** Uncertainty, by its very nature, is a difficult subject. Indeed as Davis and Keller (1997) note, even the terminology is often unhelpful:

> The self-referential problem of uncertainty about uncertainty terminology has been a notable stumbling block in this avenue of inquiry.

A useful step forward here is the typology for uncertainty in geospatially referenced information presented by Thomson et al. (2005) (building on earlier work in standardization bodies—see USGS 1977). They distinguish nine categories in their typology: accuracy/error (these are often confusing, and used interchangeably to refer to difference between observed and true or modeled values, but in this typology are sensibly combined as a single category), precision (exactness of measurement), and a number of more qualitative categories—completeness, consistency, currency/timing, credibility, subjectiveness and interrelatedness. A final category, lineage, covers the provenance information associated with a dataset. Although this typology is specific to geovisualization, it would be a useful exercise to extend it to the wider area of scientific data visualization—looking perhaps at further issues introduced by the multiple simulations of ensemble computing.

**Uncertainty information is presented in different ways** In scientific visualization, we are normally presented with a dataset (assuming scalar data for simplicity) $f_i(x_1, \ldots, x_n)$, $i = 1, 2, \ldots, m$, being unique values at a given set of $m$ points in $n$-dimensional space. The additional uncertainty information may be supplied in different ways:

**as a PDF** Rather than a unique value $f$, statistical analysis may have resulted in data at each point being provided as a random variate, $F$ say, with Probability Density Function (PDF), $g(F)$, where

$$Pr(a \leq F \leq b) = \int_a^b g(f)df$$

**as multivalue data** If the data results from several simulations as in ensemble computing, or from several physical measurements of the same entity, then we will have many values at each datapoint. That is, we will have $p$ values at each point:

$$f_i^j(x_1, \ldots, x_n), \quad j = 1, 2, \ldots, p$$

This data can then be passed for visualization as a multivalued dataset, or a PDF can be estimated from the data (in which case we generate a PDF, and we have the case above).

**as bounded data** Sometimes the data may be given simply as falling within finite bounds. Olston and Mackinlay (2002) refer to this as bounded uncertainty to contrast with statistical uncertainty, where we do not know bounds but we know the probability distribution, typically normal with mean and standard deviation (i.e. the PDF case above).

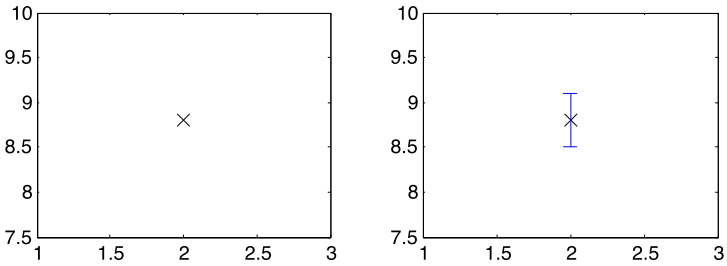


**Fig. 6.2** Error bars add a dimension: the point becomes a line

**Uncertainty propagates** When we calculate with uncertain data, we propagate the uncertainty. In the pipeline of Fig. 6.1, the original data goes through a number of transformations before an image is created. We need to understand how to propagate uncertainty in the data, through to uncertainty in the image. Careful mathematics and statistics are required, and a good primer is the NPL report by Cox and Harris (2004). The propagation problem can be stated formally as follows: given a model $Y = g(X)$ where $X = (X_1, \ldots, X_n)^T$, and the Probability Density Functions $f_{X_i}(x_i)$ for the input quantities $X_i$, with $i = 1, \ldots, n$, determine the PDF $f_Y(y)$ for the output quantity $Y$. Occasionally this can be solved analytically, but often a Monte Carlo approach is required.

In the context of visual analytics, Correa et al. (2009) describe uncertainty propagation for two common data analysis operations: Principal Components Analysis and clustering using k-means.

**Uncertainty adds a dimension to the visualization** The most elementary example will illustrate this. A single data point (2, 8.8) is plotted in Fig. 6.2—the marker is zero-dimensional, i.e. a point. But if there is uncertainty in the $y$-value, say $8.8 \pm 0.3$, then adding an error bar increases the dimension by one, as the marker becomes a line. (The *dimension of the data* remains the same—i.e. zero—but we have required an extra dimension *in the visualization* to display the additional uncertainty variable.) Similarly we shall see that isolines with uncertainty become areas, and isosurfaces become volumes. For lower dimensions this poses little problem—but on a two-dimensional display surface, we have enough problems visualizing exact 3D or higher dimensional data without introducing another dimension for uncertainty.

Even if we do not increase the spatial dimension, we still need to find a 'dimension' from somewhere. Various ideas have been tried with varying degrees of success:

**juxtaposition** A common approach is to provide a visualization of the uncertainty in a separate picture, alongside a standard representation (perhaps showing a standard deviation plot alongside a mean value plot). See for example Aerts et al. (2003).

**animation** A number of authors have used animation, making use of time as an extra dimension. A simple example is to replace the above juxtaposition approach with a toggle facility, where the user can swap between the normal view and a

view of the associated uncertainty. Experiments by Aerts et al. (2003) showed that in fact juxtaposition was better than toggling. Another use of animation is to display a sequence of different possible realizations of a model. For example, looking at uncertainty in Digital Elevation Models (DEMs), Ehlschlaeger et al. (1997) create a sequence of different realizations of a given DEM, and then generate in-between frames in order to produce a smooth animation showing the range of possibilities. Animation must be used carefully—Brown (2004) gives a good overview of the pitfalls, and suggests a useful 'vibration' technique, again illustrated on DEMs. In medical visualization, animation has been used by Lundstrom et al. (2007).

**overlay** With some visualizations, it is possible to overlay a visualization of uncertainty on top of the normal visualization. For example, Bingham and Haines (2006) overlay a contour map of an error field on top of a heatmap of the mean value of a multivalue dataset.

**sound** There were a number of early attempts to use sound to encode uncertainty—see Lodha et al. (1996a) and Fisher (1994). A difficulty is that sound is essentially a local feature (you get feedback on uncertainty at a point), whereas images give a global view—perhaps this explains why there seems to have been little recent work on using sound.

**colour** A number of authors have experimented with use of the hue, saturation, value components of color to encode uncertainty. See for example MacEachren (1992), and Hengl (2003) who adds white to indicate degree of uncertainty.

**Uncertainty tends to dominate certainty** In most natural visual representations of uncertainty, the greatest emphasis is placed on data of greatest uncertainty. Consider error bars: long bars correspond to high uncertainty. However as Hlawatsch et al. (2011) note in the context of fluid flow, it is sometimes areas of *certainty* that are more important.

**Uncertainty adds another discipline** Some of the best visualizations have been created by multidisciplinary teams, bringing together domain scientists, numerical analysts, visualization scientists and artists. See for example the storm cloud visualizations from NCSA (access.ncsa.illinois.edu/Stories/supertwister/index.htm). There is a further discipline to be added now: statistics is the branch of mathematics that deals with uncertainty, and we need increasing collaborations with statisticians in order to improve the rigor of uncertainty visualization.

The above reasons help to explain why visualization of uncertainty is hard. But the area of uncertainty of visualization is difficult too, perhaps for the following reason:

**Linearity adds uncertainty** Computer graphics hardware—from early graph plotters to current graphics cards—encourages the approximation of curves and surfaces by straight lines and triangles, inevitably introducing error.

## 6.4 Notation

In this section we re-visit an early attempt to classify scientific visualization algorithms by Brodlie et al. (1992). This work saw data as discrete items being sampled from some underlying entity, and visualization as the process of viewing a continuous empirical model built from the data. The classification was based on the dimensions of the independent variable (often spatial or temporal), and the type of dependent variable—point, scalar, vector or tensor. The classification has since been extended by a number of authors, notably Tory and Moeller (2004) who have extended the work to information visualization, and Pang et al. (1997) who used it for uncertainty visualization classification.

An $E$ notation was introduced in the 1992 paper, with a subscript indicating the number of independent variables and a superscript indicating the type of dependent variable. Thus:

$$E_1^S$$

represented a model of a scalar function of one variable, such as temperature measured over time. In the case of multifield data, where there are several variables at a datapoint, the notation extends to, for example:

$$E_1^{kS}$$

for $k$ variables, such as temperature, pressure, .... In the original work, the character $E$ had no real meaning (other than underlying Entity) and was redundant. With serendipity, we now interpret it as 'Exact', to act as a notation for *certain* data. For *uncertain* data, we simply replace $E$ by $U$.

Table 6.1 organizes the main visualization algorithms according to this classification. We subdivide the scalar class into three distinct approaches: *embed*, where we place the visualization into a higher dimensional display space (e.g. a surface view where we view a 2D data set in a 3D space); *dense*, where we view the data at every point in the domain; and *sparse*, where we extract an important feature such as a contour line. For vector visualization, we follow the subdivision suggested by Post et al. (2003): *direct*, *dense*, *geometric* and *feature-based*. The table is not complete—there are many more visualization techniques to include—but it acts as a roadmap for the techniques that have been enhanced to include uncertainty and are discussed in this article.

## 6.5 Visualization of Uncertainty

### *6.5.1 Introduction*

In this section we review the efforts that have been made to extend existing 'exact' visualization techniques to cater for uncertainty information. To organize this large body of research, we use the $U$ notation of the previous section.

**Table 6.1** Classification of techniques—key: SP = Scatter Plot; PC = Parallel Coordinates; CSV = Colored Surface View

| Dim | Point | Scalar $E/U^S$ | | | Multifield | Vector $E/U^V$ | | | |
|---|---|---|---|---|---|---|---|---|---|
| | $E/U^P$ | embed | dense | sparse | $kE/U^S$ | direct | dense | geometric | feature |
| $E/U_0$ | | Point | | | SP & PC | | | | |
| $E/U_1$ | Markers | Graph | Col Line | | | | | | |
| $E/U_2$ | | Surface view | Heatmap | Contour | CSV | Glyphs | LIC | Particles | Topology |
| $E/U_3$ | | | Vol Render | Isosurface | | | IBFV | Streamlines | |

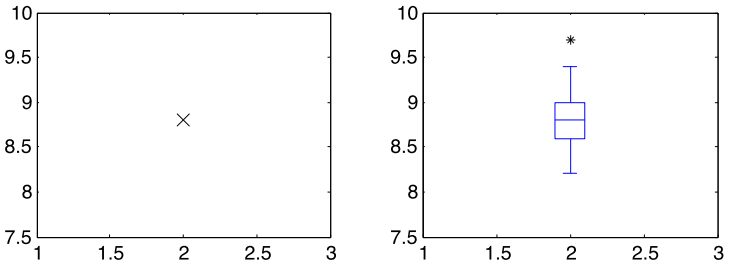


**Fig. 6.3** Tukey box plot—*on left*, a single point represents the exact observation; *on right*, the uncertainty of multiple observations is summarized as rectangle, line and outlier point, an increase of display dimension

### *6.5.2 Point Data $U^P$*

Occasionally the underlying entity is simply a collection of points in nD space, with no dependent variable associated with the points. An example in 3D would be the positions of stars in the universe, which are typically described in terms of a distance component (along line of sight from earth) and equatorial coordinates $(RA, Dec)$ to describe the direction. Li et al. (2007) consider this very problem: uncertainty in distance is much greater than in $RA/Dec$, and so error bars on the line of sight are possible, or an ellipsoid centered on the star if the $RA/Dec$ component is important.

### *6.5.3 Scalar Data $U^S$*

#### 6.5.3.1 Zero Dimensional Data $U_0^S$

This is the very simple case: with exact data, we are just plotting one point! In the uncertain case, we are typically presented with many observations of a single scalar variable. A standard uncertainty visualization is the boxplot proposed by Tukey (1977), showing the five summary statistics of upper and lower bounds, upper and lower quartiles and median. See Fig. 6.3 which takes the data point of Fig. 6.2 and assumes now that a large number of measurements have been made—notice the dimensionality increase in the visualization as uncertainty is added—rectangle, lines and outlier point rather than just a point (arguably the rectangle is only 1D as its width is not significant). There have since been many extensions and modifications (see Potter et al. 2010 for a review, and suggestion of a summary plot which incorporates further descriptive statistics such as skew and kurtosis). Cumming et al. (2007) provide important guidelines for the use and interpretation of error bars.

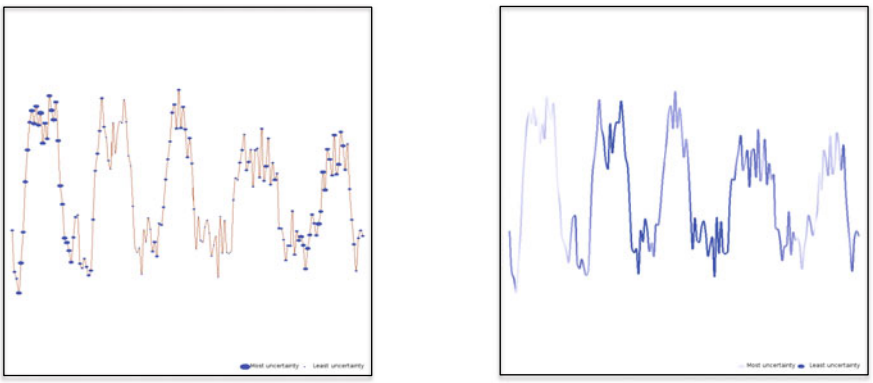


**Fig. 6.4** Examples from Sanyal et al. (2009) user study: (**a**) glyph size; (**b**) graph color. Images kindly created for this article by J. Sanyal and R.J. Moorhead

#### 6.5.3.2 One Dimensional Data $U_1^S$

**Embed—Graph** This is the ubiquitous one-dimensional graph—probably the most common of all visualizations. There are a variety of ways that an indication of uncertainty can be added: error bars can be added to the data point markers, or the markers themselves can encode the uncertainty through size or color of the glyph. A continuous model of uncertainty can be provided by color coding the graph itself, using an uncertainty color map. Sanyal et al. (2009) compare different approaches: their user study found different methods were best depending on whether the task was to locate least uncertainty (glyph size best) or highest uncertainty (color best). Figure 6.4 shows two examples from their study: showing uncertainty by glyph size and by graph color, in the latter case using different levels of saturation of blue following the early suggestion of MacEachren (1992).

#### 6.5.3.3 Two Dimensional Data $U_2^S$

**Embed—Surface Views** When surface views are used, the third space dimension is used for the visualization itself, and so another 'dimension' is needed for uncertainty. The time dimension is commonly used and animated effects are described by Ehlschlaeger et al. (1997) and Brown (2004).

Sanyal et al. (2009) do a similar study as for 1D graphs mentioned above. They examine adding glyphs at the data points on the surface, varying size and color; adding error bars to the surface; and color mapping the surface with an uncertainty measure. Here surface color worked well, except for counting of uncertainty features—where possibly perception of the shape of the mean surface was affected by the uncertainty color mapping.

**Sparse—Contouring** There are two distinct approaches to the visualization of uncertainty in contouring. The first is to draw a crisp isoline of the mean, and overlay some indication of uncertainty of the data, say standard deviation. The second is to draw some indication of the spread of contour lines that is possible for a given threshold. The first is showing uncertainty in the value of the *dependent* variable, along the mean contour; the second is showing the uncertainty in the space of the *independent* variable, for a given threshold. We call the first *value uncertainty*, and the second *positional uncertainty*.

Value uncertainty is explored in Sanyal et al. (2010). They draw uncertainty ribbons in which the thickness of the 'mean' contour lines gives an indication of the relative uncertainty at that point on the contour. Another possibility (not tried to our knowledge) is to simply color the contour lines with a measure of the value uncertainty.

Positional uncertainty has been studied by a number of researchers. The standard approach of meteorologists for example is to draw a spaghetti plot, in which a contour line is drawn for each model in an ensemble. Sanyal et al. (2010) and Potter et al. (2009) describe the use of spaghetti plots—the former comparing spaghetti plots with uncertainty ribbons, and discussing the merits of value and positional uncertainty visualization. Juang et al. (2004) use juxtaposition to look at contour plots from different realizations of a model.

Allendes Osorio and Brodlie (2008) take an image-based approach to positional uncertainty, identifying pixels where the probability of a value close to the contour threshold is sufficiently high. This gives a contour band—an area rather than a line, showing again the dimension increase that comes with uncertainty visualization. In contrast to the uncertainty ribbons in Sanyal et al. (2010), the width of the band indicates positional rather than value uncertainty. In a further variation, by mapping the probability to intensity, a fuzzy contour effect is produced, with high intensity indicating high probability of a contour passing through the pixel.

Pöthkow and Hege (2010) describe a similar method: from a set of gridded data, defined as random variates with associated PDF, they interpolate to gain a PDF defined continuously over the domain; at any point, they calculate the probability of taking two samples from the distribution, and having one sample greater than the contour threshold, and the other less. This too gives a fuzzy contour effect. The method depends on the assumption that the data at grid points is independent. This is rarely the case: in an ensemble situation, if the value from one model at a data point is greater than the ensemble mean, then it is likely that the model will similarly be above the mean at adjacent datapoints. Therefore in a subsequent paper Pöthkow et al. (2011) take the spatial correlation of the data into account; the effect is to sharpen the areas of uncertainty.

There is one further method which does not fall neatly into either category. Love et al. (2005) consider the situation where it makes sense to regard not just the data as a random variate, but also the threshold. They look for the greatest similarity between the distributions of data and the distribution of threshold. These give edge intersections which are linked as in normal contouring.

In order to illustrate some of these ideas, we make use of an oceanography case study, described by Bingham and Haines (2006). The study of Ocean Dynamic

**Fig. 6.5** Contour band: This shows the extent of the 95 % confidence interval for the zero contour, with the zero contour for the average data at each point shown for comparison

Topography (ODT), the height of the sea surface above its rest state (the geoid), is of importance to oceanographers, as it allows them to understand the circulation patterns of oceans and the associate surface currents, one of the main players in the regulation of the Earth's climate. Calculation of the ODT is difficult and so scientists focus on computation of the associated Mean Dynamic Topography (MDT). Several models for calculation of the MDT exist; Bingham and Haines collected data from eight such models, allowing them to calculate an average value, together with a formal estimate of the error. In their paper they use an overlay approach, in which the contours of the average MDT are overlaid on a heatmap of an error field. We shall use a simple method for positional uncertainty, and apply it to this problem, working directly with the ensemble data rather than estimating PDFs. Since we can interpolate each model, we assume we have values for each model everywhere in the domain. At any point, we will wish to test the null hypothesis that the data comes from a distribution whose mean value equals the contour threshold, say zero: i.e.

$$H_0 : m = 0$$

The alternative hypothesis is non-directional:

$$H_1 : m \neq 0$$

A t-test is applied to test the hypothesis and leads to two uncertain contour representations: a contour band, similar to that of Allendes Osorio and Brodlie (2008), where the 95 % confidence interval is displayed, that is, all points where the null hypothesis would not normally be rejected (see Fig. 6.5); and a fuzzy contour, where the value of the t-statistic is mapped to a color scale between sea-blue and black, giving an inky effect (see Fig. 6.6). For comparison, Fig. 6.7 shows a spaghetti plot of all eight models. (Note that we only do the calculation at points where we have data from all eight models—hence the 'unusual' geography in places!)

Finally note that it would be possible to combine both positional and value uncertainty in a single representation—for example by modifying the contour band

**Fig. 6.6** Fuzzy contour: This shows the value of the t-statistic from the hypothesis test with a color mapping from sea-blue to black based on the size of the t-statistic

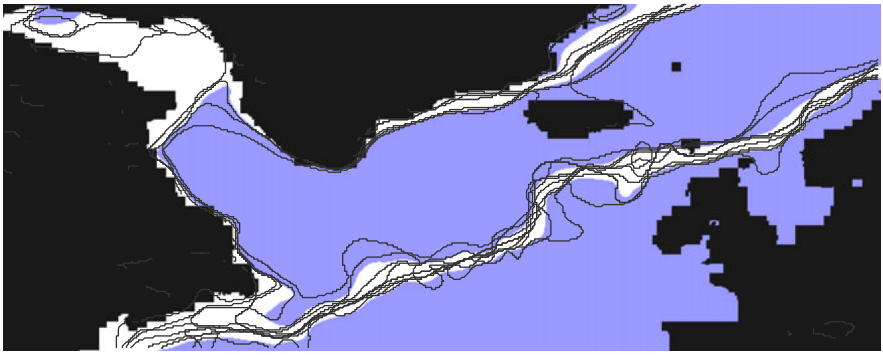

**Fig. 6.7** Spaghetti plot: zero contours from each of the eight individual models, superimposed on 95 % confidence band

shown in white in Fig. 6.5 so that a measure of the value error (say, standard deviation) was color mapped on to the band.

**Dense—Heatmap** A heatmap uses color mapping (sometimes called pseudocoloring) to visualize a scalar function over a 2D region. Various approaches have been suggested for uncertainty: a straightforward idea is to map uncertain data to a derived scalar such as mean or standard deviation (see for example Love et al. 2005); Hengl (2003) suggests addition of whiteness in areas of uncertainty; Cedilnik and Rheingans (2000) superimpose a grid where the grid lines are subtly modified to indicate uncertainty (for example, through mapping uncertainty to an intensity/width combination); Coninx et al. (2011) add Perlin noise effects.

#### 6.5.3.4 Three Dimensional Data $U_3^S$

The problem gets harder! The three space dimensions are already in use for the normal, 'certain', visualization, either by isosurfacing or volume rendering, and so the uncertainty problem becomes challenging. Embedding is no longer an option.

**Sparse—Isosurface** The approaches here mirror those for contouring. Again there is a choice between visualization of value uncertainty (mean isosurface with indication of uncertainty in data), or positional uncertainty (indication of the spread of isosurfaces possible for the defined threshold).

For value uncertainty, the 'mean' isosurface can be enhanced with an indication of uncertainty, either through color (Rhodes et al. 2003) or glyphs (Newman and Lee 2004). Grigoryan and Rheingans (2004) displace surface points in the direction of the surface normal, by a distance proportional to the uncertainty.

Positional uncertainty of isosurfaces has been addressed by the same researchers who studied positional uncertainty in contouring, as the extensions are straightforward: see the thesis of Allendes Osorio (2010), and the papers by Pöthkow and Hege (2010) and Pöthkow et al. (2011), the second incorporating spatial correlation. The fuzzy contours from the 2D case become fuzzy regions in 3D. Perception gets harder as the dimensionality increases, and the addition of a crisp, opaque isosurface of the mean of the data is necessary. Figure 6.8 shows uncertain isosurfaces using the methods of Pöthkow and Hege (2010) and Pöthkow et al. (2011): in (a) the isosurface is drawn without taking spatial correlation into account, while in (b) the use of spatial correlation gives a more localized spatial distribution of the uncertain isosurface.

Zehner et al. (2010) look at both value and positional approaches: in their value method, they extend Hengl (2003) idea of saturation mapping to indicate standard deviation; in their positional method, they construct three isosurfaces (mean, upper and lower bounds of a confidence interval), drawing the mean isosurface plus rays emanating from this to the upper and lower surfaces. Finally Love et al. (2005) extend their contour method that matches a target distribution for the threshold with the distribution of the data.

**Dense—Volume Render** This is a rather difficult technique to extend, since it already uses all three space dimensions plus color and opacity. Early work by Djurcilov et al. (2002) explored two approaches: first, the transfer function used in volume rendering was modified to map data to color and uncertainty to opacity; second, a post-processing step was added to incorporate special effects (holes, noise, texture) in areas of uncertainty.

Not surprisingly, the time dimension has also been exploited, for example by Lundstrom et al. (2007). Their application is to medical visualization where they note different transfer functions (used because the classifications are uncertain) may give different indications of how wide a vessel might be. Clinicians will generally try different preset transfer functions in order to make a decision on the stenosis. Lundstrom et al work from a probabilistic classification model, where explicit material probabilities are assigned to each CT value. An animation is then produced where areas of confident tissue classification appear static, while uncertain parts

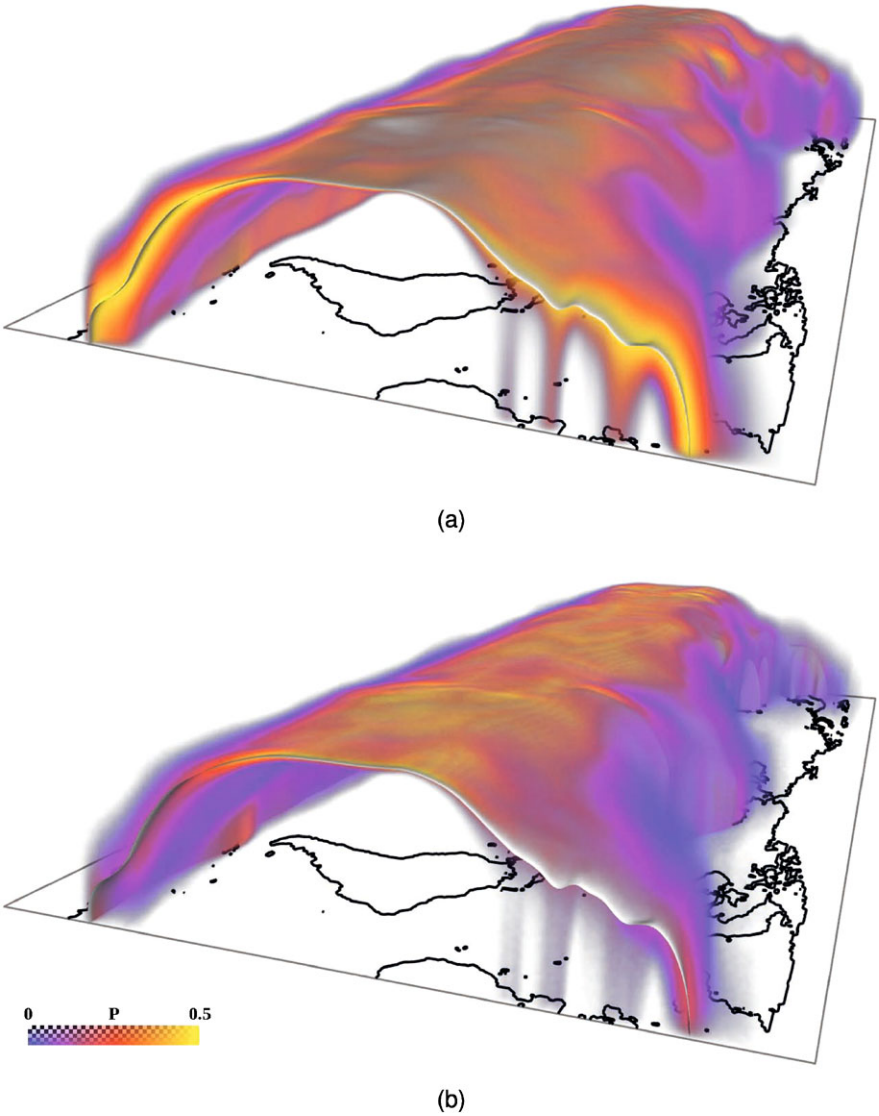


**Fig. 6.8** Uncertain isosurfaces: these are drawn using the methods of Pöthkow and Hege (2010) and Pöthkow et al. (2011): in (**a**) the isosurface is drawn without taking spatial correlation into account, while in (**b**) the use of spatial correlation gives a more localized spatial distribution of the uncertain isosurface. We are grateful to the authors for permission to use this picture which first appeared in Pöthkow et al. (2011)

change with time. In a user trial, radiologists came close to performing as well with the single animation, as with lengthy experimentation with different transfer functions.

Segmentation uncertainty is also considered in Kniss et al. (2005) and Prabni et al. (2010).

### 6.5.4 Multifield Scalar Data $kU^S$

#### 6.5.4.1 Zero Dimensional Data $U_0^{kS}$

This is the case of multivariate data where we have measurements of a set of variables, but no specific dependency on space, time or anything else. It is often visualized as a scatter plot, but is essentially a different datatype to $U^P$. Parallel coordinates is another popular technique. Uncertainty has been incorporated into scatter plots and parallel coordinates by Xie et al. (2006) who compare different visual encodings such as hue, and by Feng et al. (2010), who use density plots based on representing the data as PDFs.

#### 6.5.4.2 Higher Dimensional Data $U_{>0}^{kS}$

There is increasing interest in the visualization of multifield data defined over 2D and 3D domains, sometimes with time as an additional dimension—see for example, Jänicke et al. (2007). It is not easy to find visualizations that represent sensibly in a single picture a number of separate variables.The addition of uncertainty makes the problem even harder. Consider for example one of the simplest cases of multifield visualization, where we use a surface view to depict a 2D dataset, with height representing one variable and color representing another. The use of color for the second variable prohibits us using color for uncertainty information about the first variable, as mentioned earlier in Sect. 6.5.3.3. This is an interesting challenge. Advances in multifield visualization may help uncertainty visualization (because an uncertainty measure such as standard deviation can be treated as an extra variable), and vice versa.

### 6.5.5 Vector Data $U^V$

#### 6.5.5.1 Two Dimensional Data $U_2^V$

**Direct—Glyphs** Glyphs in the form of arrows provide a simple 2D vector visualization technique, especially for steady flows. Wittenbrink et al. (1996) consider carefully the design of uncertainty glyphs, proposing an arrow shape that widens to indicate uncertainty in bearing, with extra arrow heads for uncertainty in magnitude. Zuk et al. (2008) re-visit the topic for dense, bi-directional fields.
For unsteady flow, glyphs can be animated but the load placed on the human memory is considerable, and certainly challenging when uncertainty is added.

Hlawatsch et al. (2011) suggest a static glyph representation for unsteady flow: a glyph in the form of a small curve is traced out in polar coordinates at each data point, with the direction mapped to angle, $\theta$, and time mapped to radius, $r$. For uncertainty, curves can be drawn for the upper and lower bounds of the sequence of angles over time, and the area between the curves shaded to give an indication of the range of directions at each data point.

**Geometric—Particle Advection and Streamlines** Euler's equation gives a very simple (but not always accurate) means of calculating particle paths in a flow field:

$$x_{n+1} = x_n + v(x_n) * \Delta t \tag{6.1}$$

where $x_n$ is position at time step $n$, $v(x)$ is the velocity at $x$ and $\Delta t$ is the time-step. With uncertain data, we can think of $v(x)$ as a random variate with associated PDF (perhaps estimated from multivalue data). Luo et al. (2003) and Love et al. (2005) suggest a number of approaches:

1. a representative scalar can be used at each step, for example the mean of the distribution, and the particle path constructed as normal, without any indication of uncertainty
2. a set of paths (e.g. corresponding to the multiple values in case of multivalue data) are followed from the seed-point for the first time-step; then the centroid of the resulting end-points is calculated and used to initiate another set of paths, and so on
3. Equation (6.1) is interpreted directly in terms of PDFs, and generates a result at each time step which is a PDF—a simple means of adding two PDFs is suggested.

Although Euler's method is used here for simplicity, it would be straightforward to extend to, say, Runge-Kutta.

**Dense—Texture-Based Approaches** A number of important approaches use textures to give a visual impression of the flow field: either as a dense, noise-like pattern or as a sparse effect produced from a simulation of injecting dye. A leading method is Line Integral Convolution, or LIC, in which a dense texture is created by considering a random noise pattern, and integrating the noise forwards and backwards along streamlines through a pixel. The effect for surface velocity in the ocean example of Sect. 6.5.3.3 is studied in Allendes Osorio and Brodlie (2009). They explore different ways of encoding uncertainty within LIC: by varying the frequency of the noise pattern (low frequency—giving blur—is used for high uncertainty); with color, by assigning hue to uncertainty, and lightness to normal LIC; and by adding fog to indicate uncertainty. Figure 6.9 shows the effect of coloring the LIC.

Another popular texture approach is based on semi-Lagrangian texture advection. An example is Image-Based Flow Visualization (IBFV), in which texture is advected by the flow field and a visualization created by blending successive frames to show flow lines. Allendes Osorio (2010) explores the use of multiple frequencies (as in LIC); he also connects the opacity used in blending with the level of uncertainty in order to blur flow lines in areas of high uncertainty. Similarly, Botchen et

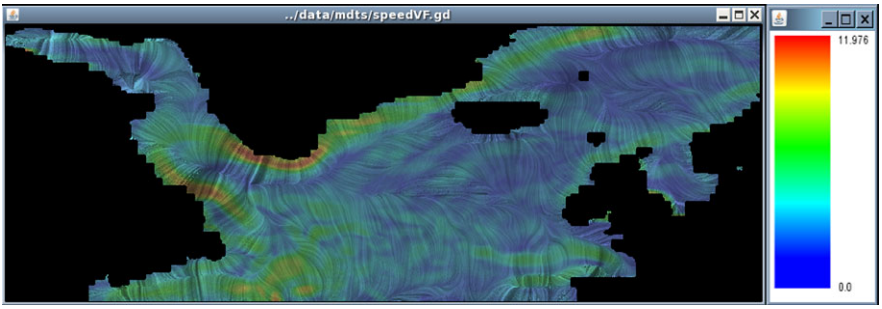


**Fig. 6.9** Uncertain LIC: here hue is used to encode the uncertainty while lightness is used to represent the LIC computation

al. (2005) explore the incorporation of uncertainty into semi-Lagrangian methods: in two of their methods, they apply a post-processing step which has a smearing effect proportional to the uncertainty—either by adding an advection perpendicular to the flow, or by diffusing in all directions; in a final method, pre-rather than post-processing, they also use multi-frequency noise. An advantage of the post-processing methods is that they work both for dense and sparse texture effects.

**Feature—Topology-Based Methods** An increasingly important set of methods focus on identifying the topological characteristics of the flow field. This enables a global view to be taken, in which critical points (zero velocity) are identified and the domain is segmented into regions with common flow behavior. Otto et al. (2010) have extended the topological analysis to the case of uncertain flow data. Faced with the particle advection difficulty of uncertain velocities in Eq. (6.1), they consider streamline integration not in terms of a single particle at point $(x, y)$ but rather a particle density function defined over the whole domain. This density function is then advected in the flow. With an initial distribution concentrated at a seed point, the integration will typically converge to a 'critical point distribution'.

#### 6.5.5.2 Three Dimensional Data $U_3^V$

The work on uncertain 2D flow visualization largely carries forward into 3D. So for example, Otto et al. (2011) extend their 2D topological analysis to the 3D case. The trajectory of stars is studied by Li et al. (2007) where cones are used to visualize the range of possible trajectories—over 50,000 years!

## 6.6 Uncertainty of Visualization

Even when we are certain about the data, we may introduce uncertainty when we generate a visualization. We take a brief look at this area now. There are two aspects: at the filter stage, we incur error when we build an interpolant from the data as an

**Table 6.2** Oxygen in flue gas

| | $x$ (time in mins) | | | | | | |
|---|---|---|---|---|---|---|---|
| | 0 | 2 | 4 | 10 | 28 | 30 | 32 |
| $y$ (% of oxygen) | 20.8 | 8.8 | 4.2 | 0.5 | 3.9 | 6.2 | 9.6 |

empirical model of the true entity; and in the map and render stages, we incur error when we represent the model in a visualization. Again we use the classification of Sect. 6.4, although Point Data in this case is trivial so we omit it.

## *6.6.1 Scalar Data $E^S$*

### 6.6.1.1 One Dimensional Data $E_1^S$

Interpolation plays a major role in scalar visualization—it lets us see not only the data but also suggests the behavior where there is no data. A simple 1D example (used before—see Brodlie 1993—but still relevant) highlights this. Consider coal burning in a furnace, with the percentage of oxygen measured in the flue gas. Data is collected at intervals of time, as shown in Table 6.2. The perils are illustrated in Fig. 6.10. The top left image shows just the data; top right is a piecewise linear interpolant—but do we really believe the rate of change of oxygen jumps dramatically at each data point?; bottom left shows a smoothly changing model, using cubic spline interpolation—but how can we have a negative percentage of oxygen?; bottom right is more credible—but still just an estimate.

### 6.6.1.2 Two Dimensional Data $E_2^S$

In 2D, bilinear interpolation dominates for rectangular gridded data. For contour drawing, this gives contour lines that are hyperbolas. Graphics systems tend to work in straight lines and so an approximation to the hyperbola is made, often very crudely by joining the intersections of the contour lines with cell edges. Lopes and Brodlie (1998) show the sort of error that can occur. The calculation of edge intersections can itself be a difficult task numerically: if the values at the end points of an edge are close to each other, and close to the threshold, the intersection calculation is ill-conditioned, as Pöthkow and Hege (2010) demonstrate.

Higher order interpolation can be used—Preusser (1989) provides a bicubic contouring routine.

If the grid is triangular, linear interpolation can be used—resulting in straight line contours.

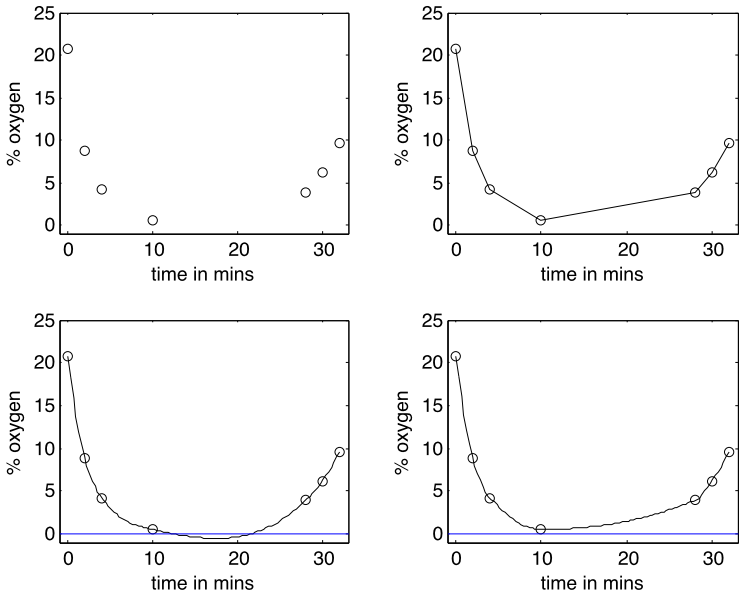


**Fig. 6.10** Perils of interpolation: oxygen burning in furnace—*top left* is data; *top right* is piecewise linear (with sharp changes in slope); *bottom left* is smooth spline, but how can a percentage be negative?; *bottom right* is a monotonic curve, credible because positive, but is minimum at 10 minutes exactly?

### 6.6.1.3 Three Dimensional Data $E_3^S$

In isosurfacing, the normal practice is to use trilinear interpolation to build an empirical model inside each cell of a rectilinear grid. This again causes difficulty further down the pipeline: the shape of an isosurface is complex and hard to represent consistently using the triangular facets required by typical graphics systems such as OpenGL (see, for example, Lopes and Brodlie 2003) who also explore issues of robustness—for example, how sensitive the representation of the isosurface is to small changes in the threshold).

Again, tetrahedral grids allow linear interpolation and triangular facet isosurfaces. Thus for rectilinear grids, it is tempting to split each cell into a set of tetrahedra in order to simplify the isosurface construction. Beware! Carr et al. (2006) nicely demonstrate the different results obtained when various different tetrahedral decompositions are used. Figure 6.11 shows the visual artifacts created from isosurfacing a test dataset; the data is sampled from a sum of nine Gaussians with most of the peaks aligned in a zig-zag pattern along the grid, the 'ground truth' isosurface being a set of spheres. Subimage (a) shows a marching cubes visualization—piecewise linear approximation to trilinear interpolation on rectangular cells; subimages (b) and (c) both show piecewise linear interpolants after cell subdivision into five tetrahedra, but doing the subdivision in two, different, equally plausible ways; subimages (d) and (e) show piecewise linear interpolants after cell subdivision into six tetrahedra,

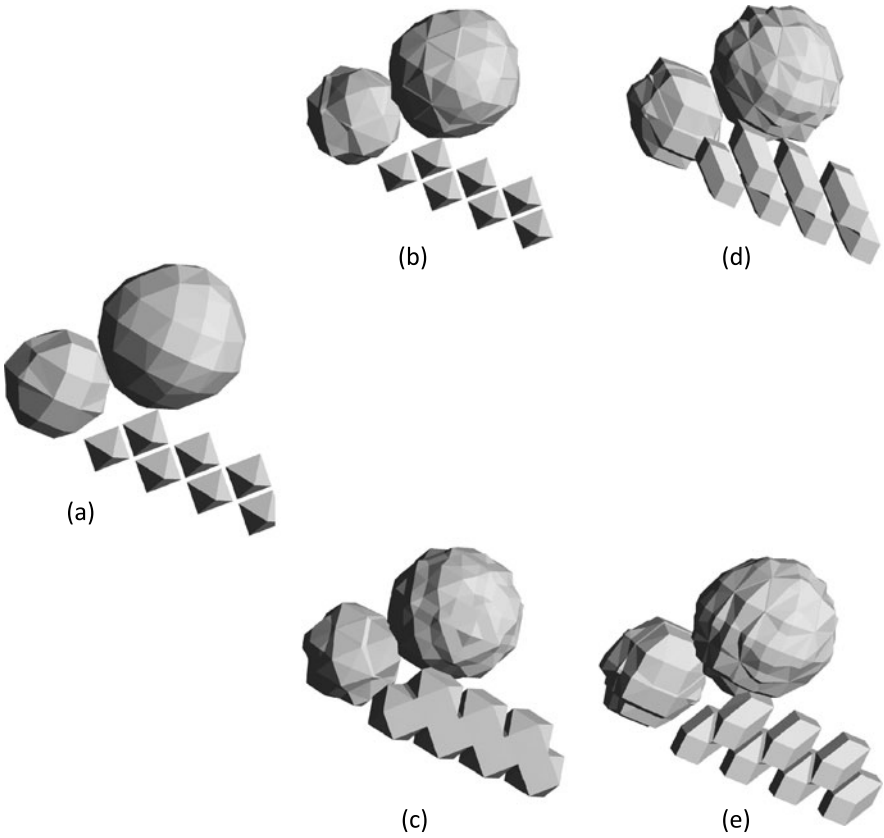


**Fig. 6.11** Effect of simplicial subdivision on isosurfaces: subimage (**a**) shows a marching cubes visualization—piecewise linear approximation to trilinear interpolation on rectangular cells; subimages (**b**) and (**c**) both show piecewise linear interpolants after cell subdivision into five tetrahedra, but doing the subdivision in two, different, equally plausible ways—notice the different topologies that result; subimages (**d**) and (**e**) show piecewise linear interpolants after cell subdivision into six tetrahedra, but using different major diagonals of the cell to do the split. Images kindly created for this article by H. Carr

but using different major diagonals of the cell to do the split. Each image (b)–(e) in Fig. 6.11 uses the same data, uses the same interpolation (piecewise linear), but shows quite different results. Further subdivisions, illustrating further artifacts, are included in the paper.

It can be frustrating for scientists who carry out simulations using higher order approximations, to find that linear approximations are required in order to visualize their results—with consequent loss of accuracy. Thus there is growing interest in being able to pass the higher order data through the visualization pipeline. For example, Nelson and Kirby (2006) show how isosurfaces can be drawn by direct ray-tracing of high order finite element data. The cost is a loss of interactivity compared with sampling on a 'fairly well-spaced' mesh and using marching cubes with

its piecewise trilinear interpolation. However Nelson and Kirby show that for high accuracy it is better to ray trace the high order data directly, than to run marching cubes on a very finely sampled mesh. Subsequent work by the authors (Nelson et al. 2011) demonstrates interactivity is possible for cut surfaces (i.e. $E_2^S$) extracted from high order finite element data, and visualized using GPU hardware; however, accurate and interactive isosurface rendering of high order data remains a challenging topic.

### 6.6.2 Multifield Scalar Data $kE^S$

Interpolation is important in design studies, where there are a number of parameters as independent variables, and a number of values that are calculated and used in multiobjective optimization. Visualization can be used to guide the optimization process by showing models of the objective functions, interpolated from sample values. Often however the calculation of a sample can be a major task, and so the data points have to be chosen with care. Wright et al. (2000) show how visualization can help steer the selection of good sample points. Berger et al. (2011) use statistical learning techniques to improve the process, and provide sensitivity analysis.

### 6.6.3 Vector Data $E^V$

For vector data, we again require interpolation. In some applications involving flow, interpolation error is a long standing issue. For example, in meteorology, Kahl and Sampson (1986) describe how substantial errors in spatial and to a lesser extent temporal interpolation can lead to false conclusions about air pollution. More recently, Boller et al. (2010) perform a study in which they aim to bound the interpolation error in each grid cell and visualize the resulting uncertainty as ribbons of varying thickness around the estimated path.

For particle advection methods, there is the additional step of numerical integration in order to calculate the path over time. Lodha et al. (1996b) explore a number of approaches to visualizing the error in the integration, such as creating a ribbon between a pair of streamlines generated by different integration methods (Euler and Runge-Kutta). Similarly, Lopes and Brodlie (1999) use the error estimates provided by NAG Library ODE solvers to provide indications of trajectory errors; Fig. 6.12 shows an envelope of trajectories formed by re-integrating with a smaller tolerance.

As in the scalar case, there is a very useful simplification for triangular or tetrahedral meshes. If we use linear interpolation in such cells, it is possible to solve the ODE analytically, removing the need for numerical integration. This idea is due to Nielson and Jung (1999), and has been further developed by Kipfer et al. (2003) and by Bhatia et al. (2011).

Accurate particle advection for high order data has been studied by Coppola et al. (2001).

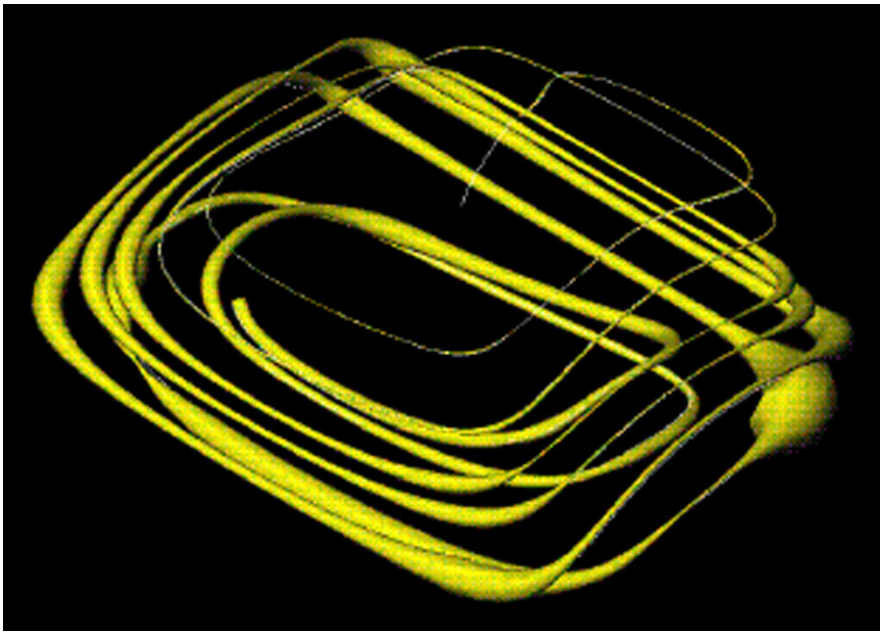

**Fig. 6.12** Uncertainty of Particle Advection: the *yellow tube* indicates an envelope within which the exact path might lie, based on integrating with different tolerances

## 6.7 Conclusions

We have reviewed the state of the art in uncertainty visualization, looking at both the visualization of uncertainty of data and also the uncertainty of the visualization process itself. We have seen that the visualization research community has enthusiastically taken up the challenge of uncertainty and most of the popular visualization techniques have been extended in some way to handle uncertain data. There is some way to go however before these techniques are standard facilities in visualization software toolkits.

A measure of the increasing interest in uncertainty visualization is that another state-of-the-art paper is underway, following discussions at a Dagstuhl seminar in 2011 (Bonneau et al. 2012); it will act as a companion paper to this review.

There remain significant research challenges ahead. While incorporation of uncertainty into 1D and 2D visualization, both scalar and vector, is relatively straightforward, there are difficult perceptual issues in adding an indication of uncertainty in 3D. There is also work to be done in linking uncertainty and risk: Daradkeh et al. (2010) for example look at the influence of uncertainty associated with the input variables of a model, on the risk associated with decision-making. In this review we have looked separately at visualization of uncertainty, and uncertainty of visualization: we need to study how both can be incorporated in a single representation.

We have mentioned that uncertainty is hard. But it is simple to ignore. Fred Brooks, in a keynote address to the IEEE Visualization conference in 1993,

reminded the audience of the need to present data honestly—while in some areas, such as realistic rendering, there is a ground truth against which the correctness of an image may be judged, in visualization we rely on the integrity of the visualization scientist. This gives us the responsibility to include in our visualizations an indication of the reliance we may place on the picture we have drawn.

**Acknowledgments** We have many people to thank: Alan McKinnon of Lincoln University, NZ, who helped us during his sabbatical at Leeds in 2009; Roger Payne, of VSNi Ltd, showed us how t-tests could help draw uncertain contours; Rory Bingham and Keith Haines who lent us the ocean data we have used in most of our uncertainty studies; Christian Hege who gave permission for us to use Fig. 6.8; Robert Moorhead, Jibonananda Sanyal and Hamish Carr who created images especially for this article; and members past and present of the VVR group at University of Leeds.

## References

Aerts, J. C. J. H., Clarke, K. C., & Keuper, A. D. (2003). Testing popular visualization techniques for representing model uncertainty. *Cartography and Geographic Information Science*, *30*(3), 249–261.

Allendes Osorio, R. S. (2010). *Visualization of uncertainty in scientific data*. PhD thesis, University of Leeds.

Allendes Osorio, R. S., & Brodlie, K. W. (2008). Contouring with uncertainty. In I. S. Lim, & W. Tang (Eds.), *Proceedings 6th theory & practice of computer graphics conference (TP.CG.08)*. Eurographics Association.

Allendes Osorio, R. S., & Brodlie, K. W. (2009). Uncertain flow visualization using LIC. In W. Tang, & J. Collomosse (Eds.), *Theory and practice of computer graphics—Eurographics UK chapter proceedings* (pp. 215–222).

Berger, W., Piringer, H., Filzmoser, P., & Gröller, E. (2011). Uncertainty-aware exploration of continuous parameter spaces using multivariate prediction. *Computer Graphics Forum*, *30*(3), 911–920.

Bhatia, H., Jadhav, S., Bremer, P.-T., Chen, G., Levine, J. A., Nonato, L. G., & Pascucci, V. (2011). Edge maps: representing flow with bounded error. In *Proceedings of IEEE Pacific visualization symposium 2011*, March 2011 (pp. 75–82).

Bingham, R. J., & Haines, K. (2006). Mean dynamic topography: intercomparisons and errors. *Philosophical Transactions of the Royal Society A*, 903–916.

Boller, R. A., Braun, S. A., Miles, J., & Laidlaw, D. H. (2010). Application of uncertainty visualization methods to meteorological trajectories. *Earth Science Informatics*, *3*, 119–126.

Bonneau, G. P., Kindlmann, G., Hege, H. C., Johnson, C. R., Oliveira, M., Potter, K., & Rheinghans, P. (2012, in preparation). Overview and state-of-the-art of uncertainty visualization. In M. Chen, H. Hagen, C. Hansen, C. Johnson, & A. Kaufmann (Eds.), *Scientific visualization: challenges for the future*.

Botchen, R. P., Weiskopf, D., & Ertl, T. (2005). Texture-based visualization of uncertainty in flow fields. In *Proceedings of IEEE visualization 2005* (pp. 647–654).

Boukhelifa, N., & Duke, D. J. (2007). The uncertain reality of underground assets. In *Proceedings of ISPRS/ICA/DGfK joint workshop on visualization and exploration of geospatial data*. ISPRS.

Brodlie, K. (1993). A classification scheme for scientific visualization. In R. A. Earnshaw, & D. Watson (Eds.), *Animation and scientific visualization* (pp. 125–140). San Diego: Academic Press.

Brodlie, K. W., Carpenter, L. A., Earnshaw, R. A., Gallop, J. R., Hubbold, R. J., Mumford, A. M., Osland, C. D., & Quarendon, P. (Eds.) (1992). *Scientific visualization—techniques and applications*. Berlin: Springer.

Brown, R. A. (2004). Animated visual vibrations as an uncertainty visualisation technique. In *International conference on computer graphics and interactive techniques in Australasia and South East Asia* (pp. 84–89).

Buttenfield, B., & Beard, M. K. (1994). Graphical and geographical components of data quality. In H. M. Hearnshaw, & D. J. Unwin (Eds.), *Visualization in graphical information systems* (pp. 150–157). New York: Wiley.

Carr, H., Moller, T., & Snoeyink, J. (2006). Artifacts caused by simplicial subdivision. *IEEE Transactions on Visualization and Computer Graphics*, *12*(2), 231–242.

Cedilnik, A., & Rheingans, P. (2000). Procedural annotation of uncertain information. In *Proceedings of visualization 2000* (pp. 77–84). Los Alamitos: IEEE Computer Society Press.

Coninx, A., Bonneau, G.-P., Droulez, J., & Thibault, G. (2011). Visualization of uncertain scalar data fields using color scales and perceptually adapted noise. In *Applied perception in graphics and visualization*. Toulouse, France.

Coppola, G., Sherwin, S. J., & Peiro, J. (2001). Nonlinear particle tracking for high-order elements. *Journal of Computational Physics*, *172*(1), 356–386.

Correa, C. D., Chan, Y.-H., & Ma, K.-L. (2009). A framework for uncertainty-aware visual analytics. In *Proceedings of IEEE symposium on visual analytics science and technology VAST 09*.

Cox, M. G., & Harris, P. M. (2004). *Uncertainty evaluation* (Technical Report). National Physical Laboratory, March 2004. Software Support for Metrology. Best Practice Guide No. 6.

Cumming, G., Fidler, F., & Vaux, D. L. (2007). Error bars in experimental biology. *The Journal of Cell Biology*, *177*(1), 7–11.

Daradkeh, M., McKinnon, A., & Churcher, C. (2010). Visualisation tools for exploring the uncertainty-risk relationship in the decision-making process: a preliminary empirical evaluation. In *Proceedings of the eleventh Australasian conference on user interface, Auic '10* (Vol. 106, pp. 42–51). Darlinghurst: Australian Computer Society

Davis, T. J., & Keller, C. P. (1997). Modelling and visualizing multiple spatial uncertainties. *Computers and Geosciences*, *23*(4), 397–408. Exploratory Cartographic Visualisation.

Djurcilov, S., Kim, K., Lermusiaux, P., & Pang, A. (2002). Visualizing scalar volumetric data with uncertainty. *Computers & Graphics*, *26*, 239–248.

Ehlschlaeger, C. R., Shortridge, A. M., & Goodchild, M. F. (1997). Visualizing spatial data uncertainty using animation. *Computers and Geosciences*, *23*(4), 387–395.

Feng, D., Kwock, L., Lee, Y., & Taylor, R. M. (2010). Matching visual saliency to confidence in plots of uncertain data. *IEEE Transactions on Visualization and Computer Graphics*, *16*(6), 980–989.

Fisher, P. (1994). Animation and sound for the visualization of uncertain spatial information. In *Visualization in graphical information systems* (pp. 181–185). New York: Wiley.

Goodchild, M., Buttenfield, B., & Wood, J. (1994). Introduction to visualizing data validity. In H. M. Hearnshaw, & D. J. Unwin (Eds.), *Visualization in graphical information systems* (pp. 141–149). New York: Wiley.

Griethe, H., & Schumann, H. (2006). The visualization of uncertain data: methods and problems. In *Proceedings of the 17th simulation and visualization conference*.

Grigoryan, G., & Rheingans, P. (2004). Point-based probabilistic surfaces to show surface uncertainty. *IEEE Transactions on Visualization and Computer Graphics*, *10*(5), 564–573.

Haber, R. B., & McNabb, D. A. (1990). Visualization idioms: a conceptual model for scientific visualization systems. In B. Shriver, G. M. Nielson, & L. J. Rosenblum (Eds.), *Visualization in scientific computing* (pp. 74–93). IEEE.

Hengl, T. (2003). Visualisation of uncertainty using the hsi colour model: computation with colours. In *Proceedings of the 7th international conference on geocomputation* (pp. 8–17). Southampton, United Kingdom.

Hlawatsch, M., Leube, P., Nowak, W., & Weiskopf, D. (2011). Flow radar glyphs—static visualization of unsteady flow with uncertainty. *IEEE Transactions on Visualization and Computer Graphics*, *17*(12), 1949–1958.

Jänicke, H., Wiebel, A., Scheuermann, G., & Kollmann, W. (2007). Multifield visualization using local statistical complexity. *IEEE Transactions on Visualization and Computer Graphics*, *13*(6), 1384–1391.

Johnson, C. (2004). Top scientific visualization research problems. *IEEE Computer Graphics and Applications*, *July/August*, 13–17.

Johnson, C. R., & Sanderson, A. R. (2003). A next step: visualizing errors and uncertainties. *IEEE Computer Graphics and Applications*, 6–10.

Juang, K.-W., Chen, Y.-S., & Lee, D.-Y. (2004). Using sequential indicator simulation to assess the uncertainty of delineating heavy-metal contaminated soils. *Environmental Pollution*, *127*, 229–238.

Kahl, J. D., & Sampson, P. J. (1986). Uncertainty in trajectory calculations due to low resolution meteorological data. *Journal of Climate and Applied Meteorology*, *25*, 1816–1831.

Kipfer, P., Reck, F., & Greiner, G. (2003). Local exact particle tracing on unstructured grids. *Computer Graphics Forum*, *22*, 133–142.

Kniss, J. M., Uitert, R. V., Stephens, A., Li, G.-S., Tasdizen, T., & Hansen, C. (2005). Statistically quantitative volume visualization. In *IEEE visualization 2005*.

Li, H., Fu, C.-W., Li, Y., & Hanson, A. J. (2007). Visualizing large-scale uncertainty in astrophysical data. *IEEE Transactions on Visualization and Computer Graphics*, *13*(6), 1640–1647.

Lodha, S. K., Wilson, C. M., & Sheehan, R. E. (1996a). LISTEN: sounding uncertainty visualization. In *Proceedings of visualization 96* (pp. 189–195).

Lodha, S. K., Pang, A., Sheehan, R. E., & Wittenbrink, C. M. (1996b). UFLOW: visualizing uncertainty in fluid flow. In R. Yagel, & G. M. Nielson (Eds.), *IEEE visualization '96* (pp. 249–254).

Lopes, A., & Brodlie, K. (1998). Accuracy in contour drawing. In *Proceedings of Eurographics* (pp. 301–312).

Lopes, A., & Brodlie, K. (1999). Accuracy in 3D particle tracing. In H. C. Hege, & K. Polthier (Eds.), *Mathematical visualization: algorithms, applications and numerics* (pp. 329–341). Berlin: Springer.

Lopes, A., & Brodlie, K. (2003). Improving the robustness and accuracy of the marching cubes algorithm for isosurfacing. *IEEE Transactions on Visualization and Computer Graphics*, *9*, 16–29.

Love, A. L., Pang, A. T., & Kao, D. L. (2005). Visualizing spatial multivalue data. *IEEE Computer Graphics and Applications*, 69–79.

Lundstrom, C., Ljung, P., Persson, A., & Ynnerman, A. (2007). Uncertainty visualization in medical volume rendering using probabilistic animation. *IEEE Transactions on Visualization and Computer Graphics*, *13*(6), 1648–1655.

Luo, A., Kao, D., & Pang, A. (2003). Visualizing spatial distribution data sets. In *Proceedings of VISSYM '03—Eurographics and IEEE TVCG symposium on visualization* (pp. 29–38). Eurographics Association.

MacEachren, A. M. (1992). Visualizing uncertain information. *Cartographic Perspective*, *Fall 13*, 10–19.

MacEachren, A. M., Robinson, A., Hopper, S., Gardner, S., Murray, R., Gahegan, M., & Hetzler, E. (2005). Visualizing geospatial information uncertainty: what we know and what we need to know. *Cartography and Geographic Information Science*, *32*(8), 139–160.

Nelson, B., & Kirby, R. M. (2006). Ray-tracing polymorphic multidomain spectral/hp elements for isosurface rendering. *IEEE Transactions on Visualization and Computer Graphics*, *12*(1), 114–126.

Nelson, B., Kirby, R. M., & Haimes, R. (2011). Gpu-based interactive cut-surface extraction from high-order finite element fields. *IEEE Transactions on Visualization and Computer Graphics*, *17*(12), 1803–1811.

Newman, T. S., & Lee, W. (2004). On visualizing uncertainty in volumetric data: techniques and their evaluation. *Journal of Visual Languages and Computing*, *15*, 463–491.

Nielson, G. M., & Jung, I.-H. (1999). Tools for computing tangent curves for linearly varying vector fields over tetrahedral domains. *IEEE Transactions on Visualization and Computer Graphics*, *5*(4), 360–372.

Olston, C., & Mackinlay, J. D. (2002). Visualizing data with bounded uncertainty. In *INFOVIS* (p. 37).

Otto, M., Germer, T., Hege, H.-C., & Theisel, H. (2010). Uncertain 2d vector field topology. *Computer Graphics Forum*, *29*(2), 347–356.

Otto, M., Germer, T., & Theisel, H. (2011). Uncertain topology of 3d vector fields. In *Visualization symposium* (pp. 67–74). IEEE Pacific.

Pang, A. T., Wittenbrink, C. M., & Lodha, S. K. (1997). Approaches to uncertainty visualization. *The Visual Computer*, *13*(8), 370–390.

Post, F. H., Vrolijk, B., Hauser, H., Laramee, R. S., & Doleisch, H. (2003). The state of the art in flow visualisation: feature extraction and tracking. *Computer Graphics Forum*, *22*(4), 775–792.

Pöthkow, K., & Hege, H.-C. (2010). Positional uncertainty of isocontours: condition analysis and probabilistic measures. *IEEE Transactions on Visualization and Computer Graphics*.

Pöthkow, K., Weber, B., & Hege, H.-C. (2011). Probabilistic marching cubes. *Computer Graphics Forum*, *30*(3), 931–940.

Potter, K., Wilson, A., Bremer, P.-T., Williams, D., Doutriaux, C., Pascucci, V., & Johnson, C. R. (2009). Ensemble-vis: a framework for the statistical visualization of ensemble data. In *Proceedings of the 2009 IEEE international conference on data mining workshops* (pp. 233–240). Los Alamitos: IEEE Computer Society.

Potter, K., Kniss, J., Riesenfeld, R., & Johnson, C. R. (2010). Visualizing summary statistics and uncertainty. *Computer Graphics Forum*, *29*(3), 823–831.

Prabni, J.-S., Ropinski, T., & Hinrichs, K. (2010). Uncertainty-aware guided volume segmentation. *IEEE Transactions on Visualization and Computer Graphics*, *16*(6), 1358–1365.

Preusser, A. (1989). Algorithm 671: Farb-e-2d: fill area with bicubics on rectangles—a contour plot program. *ACM Transactions on Mathematical Software*, *15*, 79–89.

Rhodes, P. J., Laramee, R. S., Bergeron, R. D., & Sparr, T. M. (2003). Uncertainty visualization methods in isosurface rendering. In M. Chover, H. Hagen, & D. Tost (Eds.), *Proceedings of Eurographics*. The Eurographics Association.

Sanyal, J., Zhang, S., Bhattacharya, G., Amburn, P., & Moorhead, R. J. (2009). A user study to compare four uncertainty visualization methods for 1D and 2D datasets. *IEEE Transactions on Visualization and Computer Graphics*, *15*(6), 1209–1218.

Sanyal, J., Zhang, S., Dyer, J., Mercer, A., Amburn, P., & Moorhead, R. J. (2010). Noodles: a tool for visualization of numerical weather model ensemble uncertainty. *IEEE Transactions on Visualization and Computer Graphics*, *16*(6), 1421–1430.

Thomson, J., Hetzler, B., MacEachren, A., Gahegan, M., & Pavel, M. (2005). A typology for visualizing uncertainty. In *Proceedings of the SPIE, visualization and data analysis* (pp. 146–157).

Tory, M., & Moeller, T. (2004). Rethinking visualization: a high-level taxonomy. In *Proceedings of IEEE symposium on information visualization* (pp. 151–158).

Tukey, J. W. (1977). *Exploratory data analysis*. Reading: Addison-Wesley.

USGS (1977). *Spatial data transfer standard (SDTS): logical specifications*.

Wittenbrink, C. M., Pang, A. T., & Lodha, S. K. (1996). Glyphs for visualizing uncertainty in vector fields. *IEEE Transactions on Visualization and Computer Graphics*, *2*, 266–279.

Wright, H., Brodlie, K., & David, T. (2000). Navigating high-dimensional spaces to support design steering. In *Proceedings of IEEE visualization 2000* (pp. 291–296).

Xie, Z., Huang, S., Ward, M. O., & Rundensteiner, E. A. (2006). Exploratory visualization of multivariate data with variable quality. In *IEEE symposium on visual analytics science and technology* (pp. 183–190).

Zehner, B., Watanabe, N., & Kolditz, O. (2010). Visualization of gridded scalar data with uncertainty in geosciences. *Computers and Geosciences*, *36*(10), 1268–1275.

Zuk, T. (2008). *Visualizing uncertainty*. PhD thesis, Department of Computer Science, University of Calgary.

Zuk, T., & Carpendale, S. (2006). Theoretical analysis of uncertainty visualizations. In *Visualization and data analysis*.

Zuk, T., Downton, J., Gray, D., Carpendale, S., & Liang, J. D. (2008). Exploration of uncertainty in bidirectional vector fields. In K. Börner, M. T. Grönh, J. Park, & J. C. Roberts (Eds.), *Visualization and data analysis 2008, proceedings of SPIE-IS&T electronic imaging*. Bellingham: SPIE and IS&T.